APPLICATION OF A MODIFIED SAFT-ALGORITHM ON SYNTHETIC B-SCANS OF COARSE GRAINED MATERIALS

ANWENDUNG EINES MODIFIZIERTEN SAFT-ALGORITHMUS AUF SYNTHETISCHE US-DATEN PORÖSER MEDIEN

APPLICATION D'UN SAFT-ALGORITHME MODIFIE A DES DONNEES ULTRASONIQUES ARTIFICIELLES DES MATERIAUX POREUX

Eberhard Burr, Christian U. Grosse, Hans-Wolf Reinhardt

SUMMARY

In non-destructive-testing the Synthetic Aperture Focussing Technique is frequently used [Langenberg, 1987] to get an image of the investigated specimen from ultrasonic data. Though the algorithm is applied to any kind of material, it's theory is only valid in the case of homogeneous media. That is why the results in coarse grained materials, for example in concrete, are difficult to interpret or have to be analysed with special techniques [Köhler et al., 1997]. It is shown, that the algorithm can be modified in a simple way to get better results for imaging purposes.

ZUSAMMENFASSUNG

Um sich aus Ultraschalldaten ein Bild (Image) von Rissen und Fehlstellen in einer untersuchten Probe zu machen, wird in der zerstörungsfreien Prüfung oft ein SAFT-Algorithmus (Synthetic Aperture Focussing Technique) [Langenberg, 1987] verwendet. Seine theoretische Grundlage ist im Wesentlichen für homogene Materialien gültig. Entsprechend problematisch ist die Anwendung auf Daten aus Versuchen mit porösen Medien (z.B. Beton). Solche Anwendungen erfordern deshalb spezielle Aperturen [Köhler et al., 1997]. Die Qualität des Images läßt sich allerdings

mit einem modifizierten SAFT-Algorithmus verbessern, welcher die Wahrscheinlichkeit erhöht, einen Riß zu detektieren.

RESUME

Pour se faire une idée des ruptures dans un spécimen examiné avec des méthodes ultrasoniques en essai non-destructive il y a la possibilité de prendre une SAFT-algorithme [Langenberg, 1987] (Synthetic Aperture Focussing Technique). Mais en théorie, cette algorithme est seulement applicable aux matériaux homogènes. Les résultats en matériaux poreux sont correspondant mauvais ou seulement à obtenir avec des intallations d'essai spécielles [Köhler et al., 1997]. Avec une modification de cette algorithme nous avons la possibilité d' élever la qualité des images et nous avons la chance de détecter des ruptures en matériaux inhomogènes.

KEYWORDS: synthetic ultrasonic data, inversion, imaging

1. INTRODUCTION

In the previous article of this journal [Burr et al., 1997], assumptions were made regarding the source of the ultrasonic signal and the B-Scan's were computed using the elastic wave equation - a linear differential equation - which was solved for every point of the media and which yields the displacement for every timestep of the signal at these points.

Now the inverse problem is to be solved. The data (A-Scan or B-Scan) has been detected and it is known that it can be described as an output of a linear system, but the structure of this linear system is unknown. The output of this linear system can be computed in a convolutional process. Because the spectrum of the signal $q(\vec{r}_0, \omega)$ at the place $\vec{r}_o$ with frequency ω multiplicated with the impulse response $G(\vec{r}_0, \vec{r}, \omega)$ of the medium, yields the spectrum of the displacement $u(\vec{r}, \omega)$ at the receiver place $\vec{r}$ in the data.

$$q(\vec{r}_0, \omega) * G(\vec{r}, \vec{r}_0, \omega) = u(\vec{r}, \omega)$$

With a deconvolutional process there is the possibility to conclude on the signal $q(\vec{r}_0, \omega)$. It has to be stressed, that the signal searched for isn't the source signal of the wave excitation, (this is done by acoustic emission problems) but the aim of interest is the scattering signal of the flaw scatterer excited by the incident wave. This work, the deconvolution, is well done for homogenous materials by a SAFT-algorithm, but for inhomogeneous materials the algorithm fails and yields artifacts in the image which don't match with real scatterers in the medium.

This effect can be depressed with a modified SAFT-algorithm. It is possible to influence the imaging quality of the imaging algorithm. This can be done by taking into account that the length of the flaw searched for, is much larger than the correlation length of inhomogenities that disturb the image, for example air inclusions in concrete, etc. Therefore, there is the possibility to average out the noise effects and get better images even for coarse grained materials.

2. THEORETICAL BACKGROUND

The inverse scattering algorithm SAFT is only valid for scalar waves in isotropic homogenous materials. Therefore the elastic wave equation in these materials is splitted into a scalar potential for the pressure waves and a vector potential for the shear-waves. The solution of these two potentials are plane waves with different speed. In two dimensions the vector-waves can be splitted. The first component consists of shear horizontal waves (SH) propagating along the z-axis with displacement along the x-axis (perpendicular to the propagation direction of the plane wave in Fig. 1). They are therefore uncoupled from the pressure-waves (purely scalar). The second component are shear waves with vertical displacement (SV) that are coupled with the pressure

wave. With a plane wave excitation along the x-axis, SV-waves only appear due to mode-conversion at the scatterer and the problem is mostly scalar.

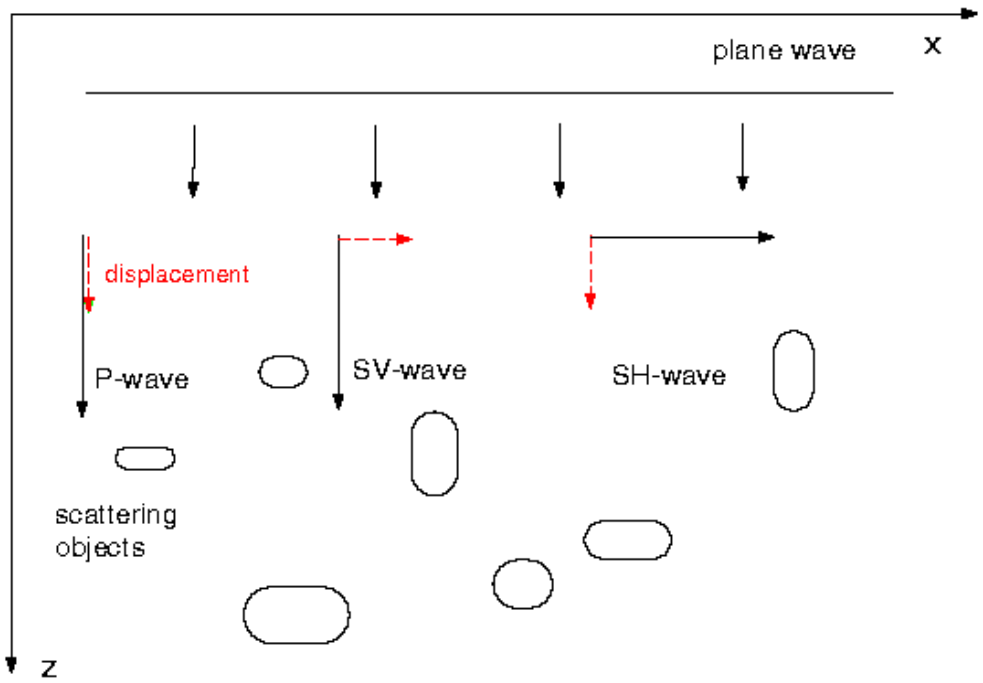

Fig. 1: *Schematic figure of different elastic wave types.*

The formulation of the spectral multiplication of the scattering signal and the impulse response of the medium in the time domain yields in a convolutional integral, where the signal $q(\vec{r}_0, t_0)$ is being replaced by a delta-pulse at a given point and a given time:

$$\delta(\vec{r} - \vec{r}_0)\delta(t - t_0)G(\vec{r} - \vec{r}_0, t - t_0)d^3\vec{r}dt = u(\vec{r}, t)$$

This means it is only searched for a pointlike scatterer. This equation can be solved for the displacement and placed into the scalar wave-equation. For the homogeneous infinitely extended two dimensional space with the velocity v_c, $u(\vec{r}, t)$ can be replaced for this kind of signal by $G(\vec{r} - \vec{r}_0, t - t_0)$.

$$(\Delta - \frac{1}{v_c^2}\frac{\partial^2}{\partial t^2})G(\vec{r} - \vec{r}_0, t - t_0) = \delta(\vec{r} - \vec{r}_0)\delta(t - t_0)$$

For $\vec{r} = \vec{r}_0$ the result is only valid for monostatic experiments, providing that the illuminating source and the receiver are coincidentally at the same place. As a result the pointlike scatterer is represented in the time domain (B-Scan) as a parabola for a plane wave excitation of the scatterer and as a hyperbola for a pointsource excitation [Langenberg, 1993]. (The pointlike scatterer being illuminated by a spherical wave or a plane wave.)

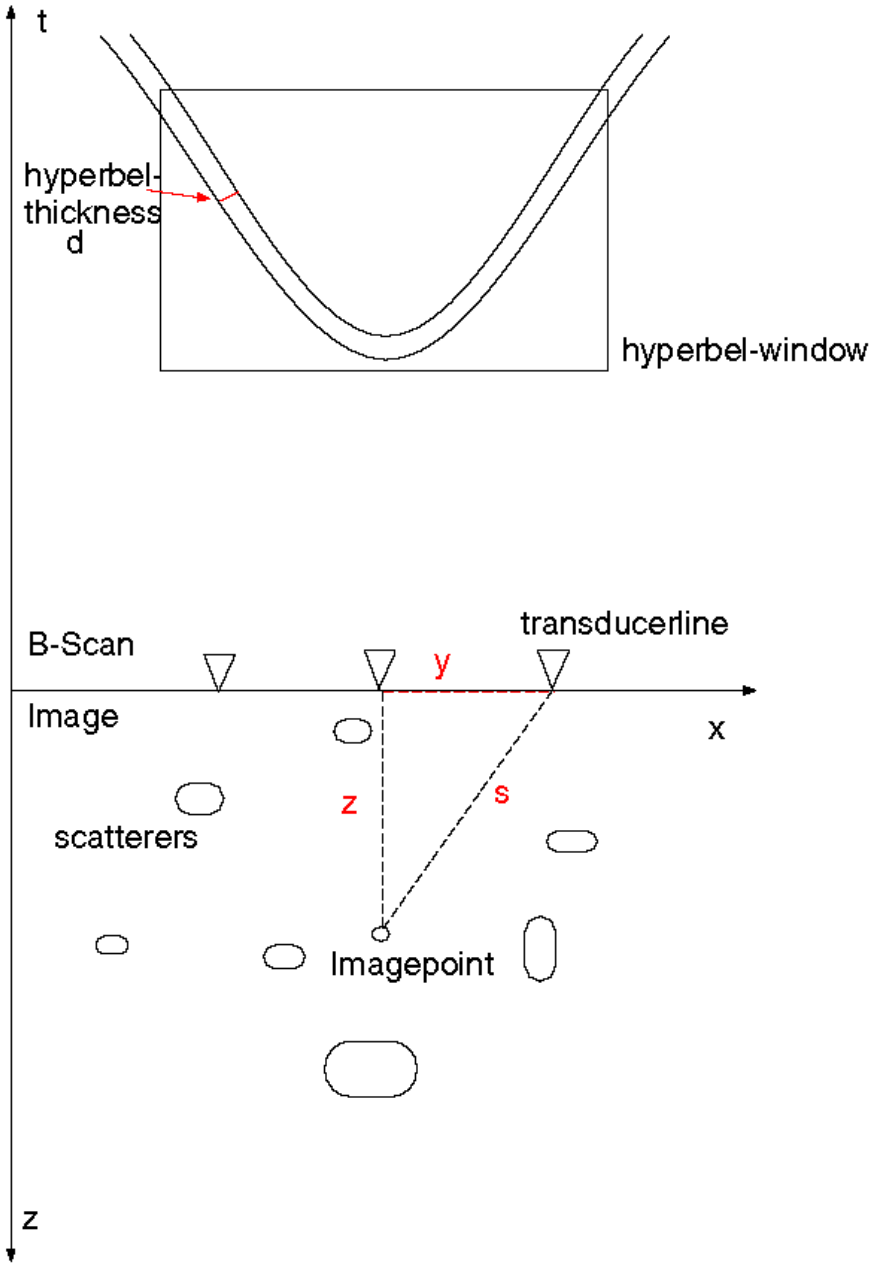

Fig. 2: *Geometrical method to find the equation of the hyperbola.*

For the pointsource there is an easy way to compute the equation for the hyperbola with geometrical methods in the time domain (Fig. 2) [Robinson, 1980]. Application of the pythagoras formula to compute the squared time of the wave from the transducer to the imagepoint and back yields:

$$t_s^2 = t_y^2 + t_z^2 = \frac{4}{v_c^{\,2}}(y^2 + z^2)$$

So the intention is to find the hyperbolas or (in this paper) the parabolas in the data-space. For every imagepoint a parabola is calculated in which the main energy is scattered. If the summation over this parabola yields a high value, a scattering point is preserved in the image. There are several parameters that are very important for the parabola, especially for imaging in inhomogeneous media (for which the theory is not valid).

The first parameter is the length of the window which contains the parabola. The algorithm gets inefficient if the parabola is placed over the whole data-array, because there are lots of size-effects and noise, which have a negative influence on the result if they are taken into account. Moreover the algorithm works much faster if there is just a small window used in which the parabola is placed.

The second parameter is the thickness d of the parabola. This value is very important, especially when dealing with inhomogeneous materials. It has the same effect as summing up traces of pointlike receivers over the diameter of a transducer [Ishimaru, 1987]. In an inhomogeneous material it is more effective to use a thicklined parabola which averages out the noise due to small inhomogenities, that isn't searched for. Therefore the image of the flaw searched for gets not as sharp as in the case using a thinlined parabola, but there aren't all the artifacts due to noise and air inclusions. With a parabelthickness d larger than the correlation length of the waves scattered due to the small inhomogenities, these fluctuations aren't taken into account in

the image. Only the flaw with a length same or bigger than the parabola-thickness is detected. Equation for the parabola with varying thickness:

$$(t_s \pm d) = 4\frac{y^2}{v_c} + 2\frac{z}{v_c}$$

The parameter d has been added to the time t because it has the highest sampling rate. Adding it to v_c or to z, it would have been difficult to get rid of the noise effects due to the coarser sampling rate, without overlooking the reflections searched for. As soon as there is an theoretical approach which relates the parabola thickness d to the correlation length of the air inclusions and the flaw, this problem shouldn't arise anymore. In the following examples v_c is always the average medium-velocity of the concrete (4 km/s), without taking the influence of the scattering attenuation of the small air inclusions on the mean wavefield ("Meanfield" [Shapiro,1993]) into account. Yet if this influence becomes too large it is reasonable to use the effective velocity of the medium.

The third parameter allows to weigh "both sides" of the parabola. Far away from the top of the parabola, the energy for the image becomes less important and many more noise-effects influence the result negatively. This fault is reduced by introducing a parameter that improves the result by dividing the datapoint through its distance from the top of the parabola. This possibility hasn't been tested so far because only a small window was chosen mostly, in comparison to the enlargement of the parabola.

To make the algorithm faster, there is also the possibility to use a picker for the amplitude. The used picker works in the following simple way: For every imagepoint a datapoint at the top of the parabola is taken and compared to an average amplitude of the whole dataspace. If the data-amplitude is, for instance, 3/4 of the averaged amplitude, the parabola is used for the summation, otherwise the next imagepoint is taken. This value is taken for every inversion presented in this paper, for the facility of comparison.

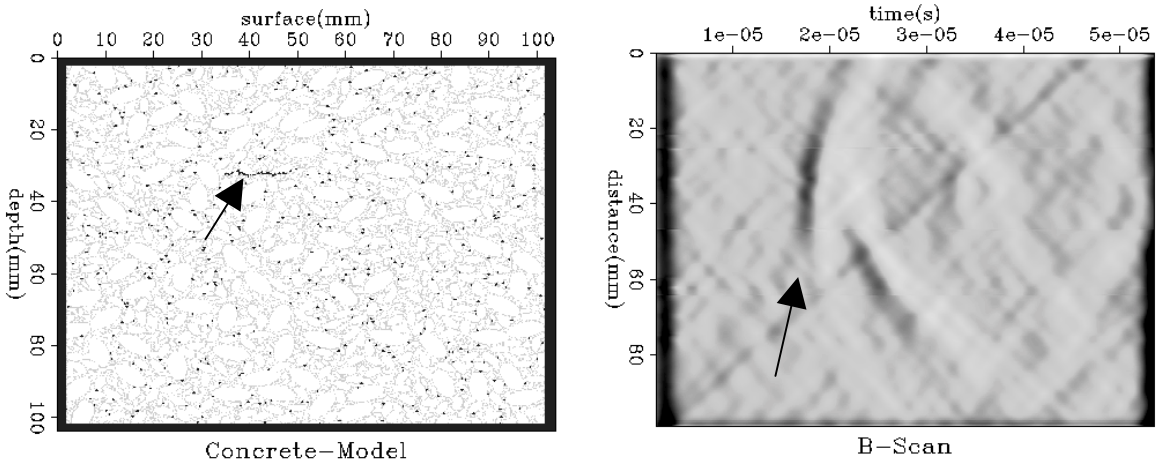

Fig. 3: *Left: Concrete Model with 1% air inside and the flaw in 3cm depth.*
Right: B-Scan of a plane wave scattered at this flaw.

3. RESULTS OF A SYNTHETIC EXPERIMENT

A plane elastic wave is send through different kind of models with a flaw inside. From an experimental point of view, this isn't a very useful simulation, because so far it is difficult to send plane waves through concrete specimens. However the plane-wave-simulations in this synthetic experiment saves lots of computation-time (only one simulation is needed for one B-Scan; in the case of a monostatic experiment there is the need of numerous F-D-simulations for one B-Scan). Another advantage is, that SV-waves take only place because of mode conversion at the scatterer and the condition for scalar wavefields is mostly fulfilled. The disadvantage of this simplification is a little loss of information for every trace, because the spatial illumination of the model is smaller. The difference in the processing-scheme is, that if there is a B-Scan of a monostatic experiment (geophysically: zero-offset shot gather) which has to be inverted, the SAFT-algorithm sums up over the hyperbolas. With the same approach and the use of a plane wave excitation, the summation takes place along the parabolas and the result becomes very similar.

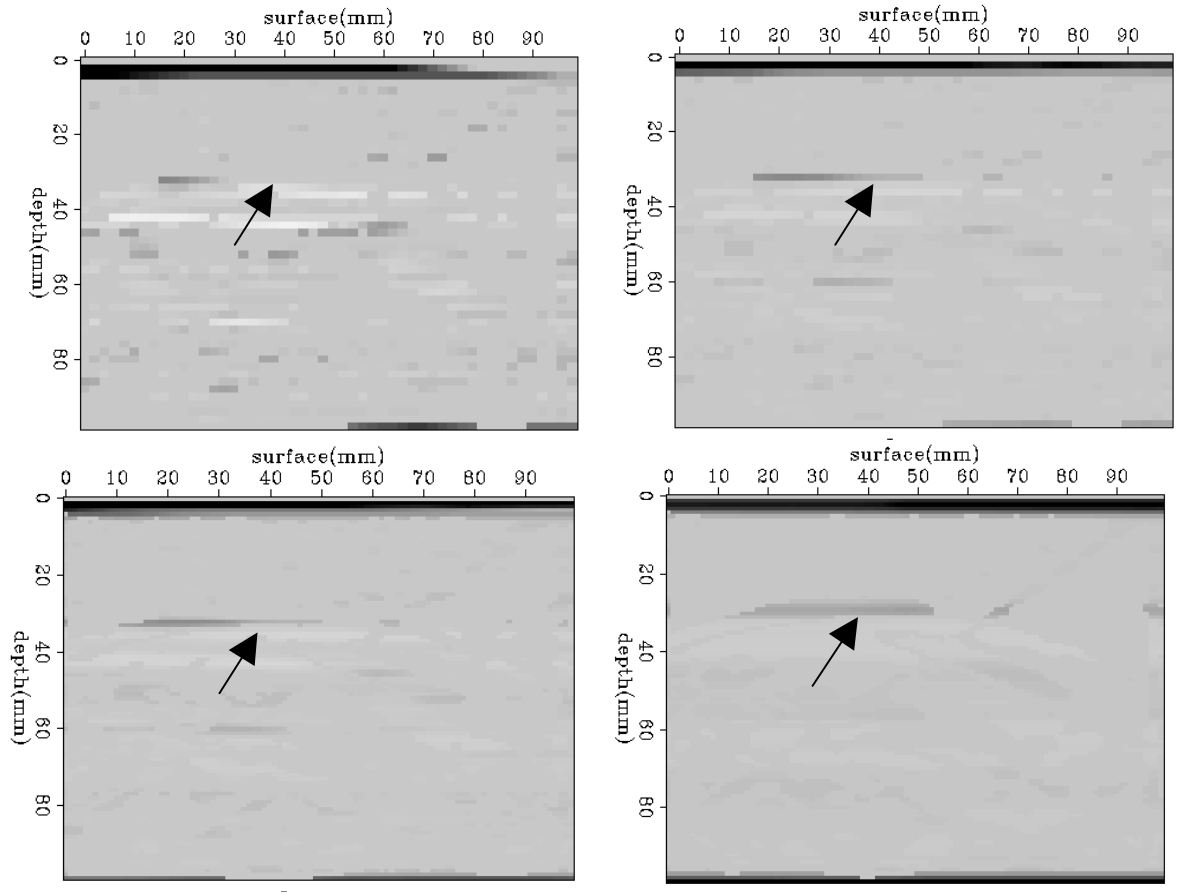

Fig. 4: *Different images of a concrete model with 1% air inside. Top left: d = 0,1, 50*50 imagepoints. Top right: d = 0,25, 50*50 imagepoints. Bottom left: d = 0,25, 100*100 imagepoints. Bottom right: d = 0,5, 100*100 imagepoints.*

Presenting some examples: Numerous simulations have been done with the purpose to receive B-Scans for the inversion. These are simulations with flaws in different depths and materials with different layouts.

The FD-simulation is always carried out in two dimensions over a model with 500 * 500 gridpoints representing a 10 cm * 10 cm specimen with reflecting boundaries. So all the size-effects of a true experiment has been included. The concrete model is almost the same as described in the previous article, with differing percentages of air inclusions. All ellipses are of the same size, the flaw is located always horizontally in different depths and is a bit smaller (only 2 cm length). The B-Scans are taken from a receiverline on top

of the model. (For further details please read the article about FD-simulations [Burr et al., 1997]).

The first simulation is carried out with only one percent air inclusions (Fig. 3). The flaw is placed at a depth of 3 cm and starts at about 3 cm on the left side. The B-scan represents the incoming plane wave on the left side. The reflection-parabola of the reflected pressure-wave is well seen after 17 µs at the surface. The shear wave arrives at 30 µs, being a factor $\sqrt{3}$ slower. After 54 µs the backwall echo is detected. Every later registration has been cut away. All the other structures in the B-Scan are due to size-effects and scattering at the ellipses with parameters of the stuffing materials and air.

The images at the top of Fig. 4 are presented at the size of 50 * 50 gridpoints. The parabola is computed with a windowlength including the whole data-array, because the algorithm worked fast enough and the parabolas reached both sides of the array. The d of the top left image in Fig. 4 is 0,1 and 0,25 of the next two images. So varying the thickness of the parabola leads to images of a different quality. As soon as little fluctuations aren't averaged out of the energy summed up for the image point, artifacts are resulting. This means that scatterers are detected at wrong positions and with wrong sizes. The images using the thicklined parabola (top and bottom right of Fig. 4) show less artifacts; those that appear are due to the fact that the shear wave is also distributing its energy to the imagepoints yet to the pressure-wave parabolas with the wrong velocities. Timegating would reduce this effect but in this example it is small enough to be ignored. There is also the possibility, that the fractal shape of the flaw is decreasing the quality of the image. An influence on the lateral position of the flaw is the result. In the images with small d the flaw is pushed to the left and in images with a thicklined parabola the flaw is too long (see bottom right of Fig. 4). The latter effect is also because a higher parameter d reduces the sharpness of the image. On the bottom left of Fig. 4 the same result for images with 100*100 imagepoints is shown. Using more pixels and the same value for $d = 0{,}25$ has the effect, that the quality of the image rises and the lateral disintegration becomes better.

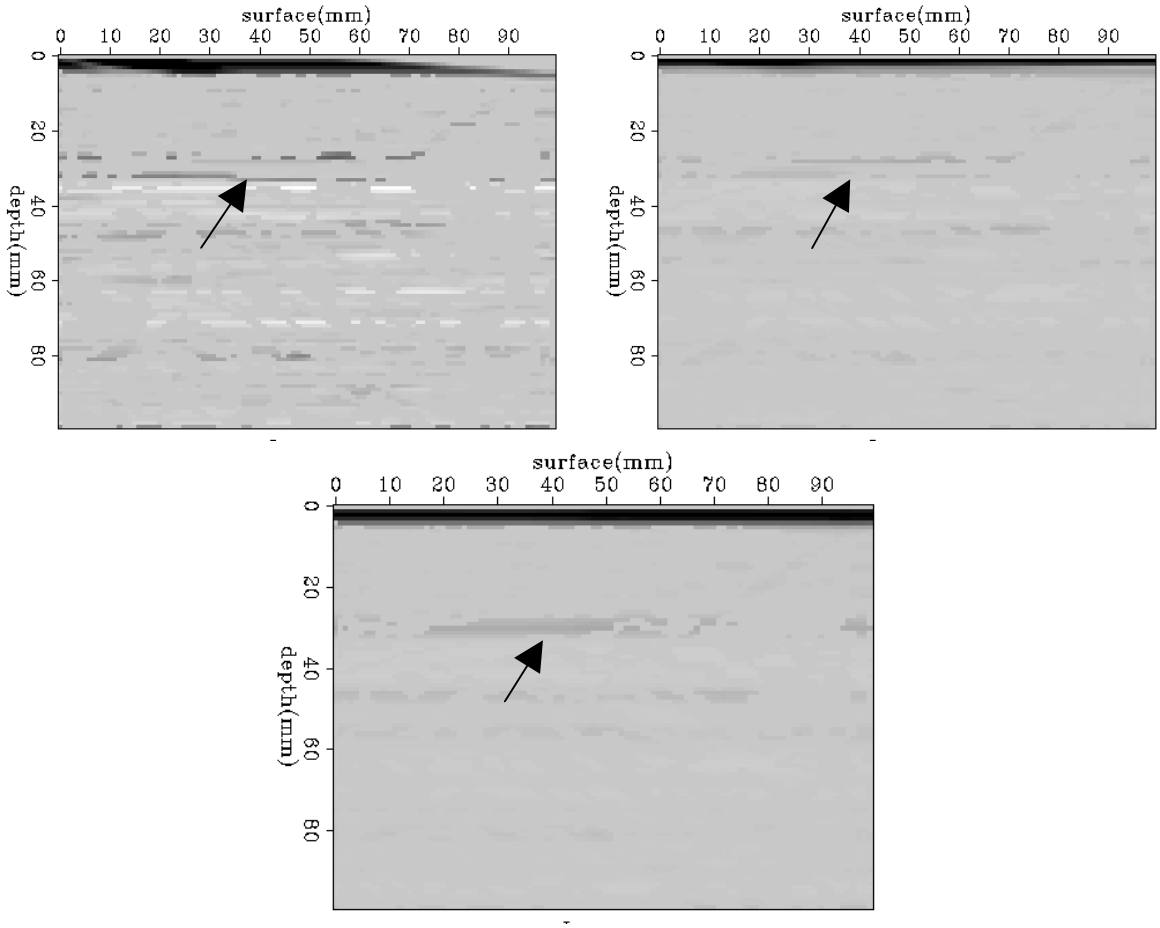

Fig. 5: *Different images of the concrete model with 2% air inside; all with 100*100 imagepoints. Top left: d = 0,1. Top right: d = 0,25. Bottom: d = 0,5.*

The same situation comes up in concrete with 2% air inclusions. The data file has more noise but the parabola is again well seen. All images in Fig. 5 consist of 100*100 gridpoints. Only the parameter d is varying. On the first picture with $d = 0{,}1$ there are lots of artifacts, the second picture with $d = 0{,}25$ isn't also very useful because there is no possibility to distinct between artifacts and flaw. The third image of the flaw with $d = 0{,}5$ has a low contrast and the position of the flaw is in the right area. Artifacts get depressed and only the lateral extend of the flaw-image is too big, because of reduced sharpness.

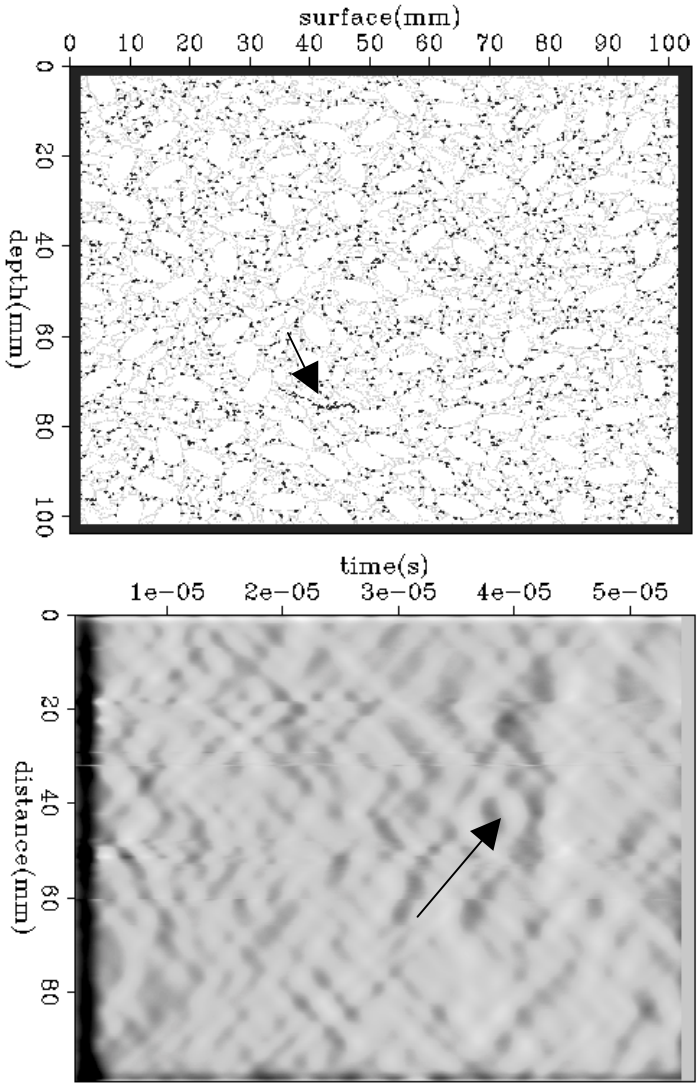

Fig. 5: *Top: More complicated model with a flaw in 7cm depth and 4% air .*
Bottom: B-Scan of a plane wave scattered at the flaw.

The last synthetic model is more complicated, while using 4% air inclusions and placing the flaw in a depth of 7,5 cm only with a length of 1 cm. In the B-Scan there is only the possibility to imagine the reflection-parabola reaching the surface after 45 µs. Cutting the backwall reflection in order to get a better quality leads to less artifacts in this case. The 100*100 gridpoints image in Fig. 6 is quite worse, but taking a closer look at it, the flaw is found in the correct depth and with the correct position. Again only the lateral extension is too big. A value of $d = 2{,}5$, has been used to get this result.

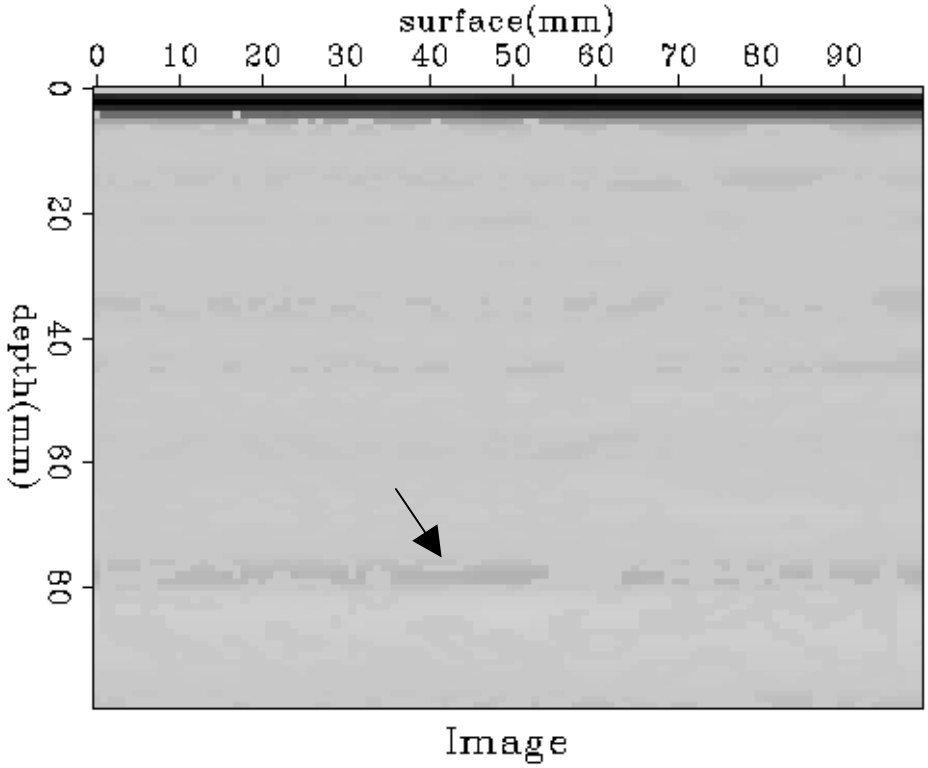

Fig. 6: *Image of our more complicated model(Fig. 5). With d = 2,5 and 100*100 Imagepoints we are able to cope with this problem.*

4. CONCLUSIONS

It is well seen that the modification of the used algorithm presents several new outlooks in the imaging of inhomogeneous media. Very important for further applications is a theoretical approach, which is able to relate the length of the flaw to be detected to the thickness of the hyperbola used.

In future this algorithm for inverting data of ultrasonic B-Scans on inhomogeneous media will be tested on synthetic materials in other sizes and flaws with different angles to the illuminating wave. In order to solve this problem it is useful to include the shear waves to the investigation and there should also be made use of time-gating to differ shear-wave from pressure-wave reflections .

Additionally is interesting to test the ability of the modified algorithm at experiments with real concrete. Yet problems like data conversion, sorting of the data (if there are no monostatic geometries) and depressing of aperture-noise and size-effects will arise. There is also the possibility to extend the algorithm to 3D-imaging.

ACKNOWLEDGEMENTS

We gratefully acknowledge funding of our work the Deutsche Forschungsgemeinschaft (DFG) in part A6 of the special research program SFB 381 „Charakterisierung des Schädigungsverlaufes in Faserverbund-werkstoffen mittels zerstörungsfreier Prüfung“.

REFERENCES

BURR, E., GOLD, N., GROSSE, C., REINHARDT, H.-W. (1997*): Simulation of Ultrasonic Flaw-Detection in Concrete with a different Percentage of Air Inclusions*, (this journal).

HERMAN, G.T., TUY, H.K., LANGENBERG, K.J., SABATIER, P. (1987*): Basic Methods of Tomography and Inverse Problems*. Adam Hilger, Bristol.

ISHIMARU, A. (1987): *Wave Propagation and Scattering in Random Media*. Vols 1 and 2. New York: Academic Press.

KÖHLER, B., HENTGES, G., MÜLLER, W. (April 1997*): A novel technique for advanced ultrasonic testing of concrete by using signal conditioning methods and a scanning laser vibrometer*. Proceedings of the International Conference 'NDT in Civil Engineering', Liverpool.

LANGENBERG, K.-J.,FELLINGER, P., MARKLEIN, R., ZANGER, P., MAYER, K., KREUTTER, T., (1993): *Inverse Methods and Imaging*. P. 317-398. Out of Evaluation of Masterials and structures by quantitative ultrasonics from J.D. Achenbach. Springer Verlag, Wien New York.

ROBINSON, E.A.,TREITEL S.(1980): *Geophysical Signal Analysis*. Englewood Cliffs, NJ: Prentice Hall.

SHAPIRO, S. A., KNEIB, G. (1993*): Seismic attenuation by scattering: theory and numerical results*. Geophysical Journal International 114, S.373-391.